Article:
Ma, Y, Chen, X orcid.org/0000-0002-2053-2448, Hosking, LJ et al. (3 more authors) (2021) The influence of coupled physical swelling and chemical reactions on deformable geomaterials. International Journal for Numerical and Analytical Methods in Geomechanics, 45 (1). pp. 64-82. ISSN 0363-9061

https://doi.org/10.1002/nag.3134

The influence of coupled physical swelling and chemical reactions on deformable geomaterials

Yue Ma[1], Xiao-Hui Chen[1*], Lee J. Hosking[2], Hai-Sui Yu[1], Hywel R. Thomas[3], Simon Norris[4]

[1]School of Civil Engineering, University of Leeds, LS2 9JT, UK

[*]Telephone: +44 (0)113 3430350

[*]Email: x.chen@leeds.ac.uk

[2]Department of Civil and Environmental Engineering, Brunel University London, Kingston Lane, Uxbridge, Middlesex, UB8 3PH, UK

[3]Geoenvironmental Research Centre, School of Engineering, Cardiff University, Cardiff CF24 3AA, UK

[4]Radioactive Waste Management, UK

Abstract:

Coupled thermo-hydro-mechanical-chemical modelling has attracted attention in past decades due to many contemporary geotechnical engineering applications (e.g. waste disposal, carbon capture and storage, etc.). However, molecular-scale interactions within geomaterials (e.g. swelling and dissolution/precipitation) have a significant influence on the mechanical behaviour, yet are rarely incorporated into existing THMC frameworks. This paper presents a new coupled Hydro-Mechanical-Chemical constitutive model to bridge molecular-scale interactions with macro-physical deformation by combining the swelling and dissolution/precipitation through an extension of the new mixture coupling theory. Entropy analysis of the geomaterial system provides dissipation energy, and Helmholtz free energy gives the relationship between solids and fluid. Numerical simulation is used to compare to the selected recognized models, which demonstrates that the swelling and dissolution/ precipitation processes may have a significant influence on the mechanical deformation of the geomaterials.

Keywords: HMC model, swelling and dissolution, precipitation, mixture coupling theory, non-equilibrium thermodynamics

1 Introduction

Swelling clay-rich geomaterials have been widely used for waste management as engineered or host barriers (e.g. nuclear waste disposal, liquid mining waste, etc.). These barriers, however, will be exposed to coupled thermal (T), hydraulic (H), mechanical (M) and chemical (C) processes, and may be strongly influenced by acidic or alkaline leachate (e.g. the hyper-alkaline leachates from the cementitious barrier of intermediate/low-level waste). Research has been conducted to study the behaviour of engineered barriers under such coupled situations (Gens et al., 2004, Liu et al., 2011, Xiaodong et al., 2011, Peter, 2011), however, little research has been done on the coupled swelling and dissolution/precipitation process.

Typically, two major swelling mechanisms present: crystalline swelling and osmotic swelling. As clay minerals have a high affinity of water, up to four layers of water molecules can be absorbed into the clay platelets and line up to form a quasi-crystalline structure, which will result in the expansion of the interlayer space (Anderson et al., 2010). Osmotic swelling results from the difference of the ion concentration in the clay platelets and in the pore fluids (Madsen and Müller-Vonmoos, 1989).

Dissolution/precipitation occurs when a clay-rich geomaterial contacts with hyper-acidic or hyper-alkaline leachate. For example, the cementitious materials which can be used as a barrier for nuclear waste disposal will produce hyper-alkaline leachates during the re-saturation process with groundwater (Savage et al., 2002). Such leachates with a pH range from 10-13.5 will react with the mineral components of the host rock, and result in dissolution/precipitation of the barrier (Berner, 1992). The mechanism and influence of such dissolution/precipitation have been explored both experimentally and numerically (Criscenti and Serne, 1988, Adler et al., 1999, Schwartzentruber et al., 1987, Berner, 1998, Hu et al., 2012, Jia et al., 2017).

Both swelling and dissolution/precipitation occur at the molecular scale and may significantly change the microstructure and components of the geomaterials, resulting in changes of macroscopic physical properties. Swelling and dissolution/precipitation have been studied extensively as individual processes, without sufficiently considering couplings between each other. The research of coupling the molecular process into THMC framework remains a

challenge. This is partly because most of the existing THMC research are based on a mechanics approach, which suffers difficulties in handling molecular-scale chemical coupling.

The mechanics approach is based on the classic consolidation theory of Terzaghi (Terzaghi, 1943) and Biot (Biot, 1962, Biot and Temple, 1972). This widely-used approach has difficulties of building the interactions between microscopic molecular force and macroscopic pressure and forces, and it has to borrow formulations from geochemistry for chemical couplings, lacking theoretically rigorous interpretation of physical-chemical coupling.

An advanced approach for THMC modelling, the mixture coupling approach, has been developed by Heidug & Wong (Heidug and Wong, 1996), and further extended by Chen et al. (Chen, 2013, Chen, 2010). This approach, based on the fundamental theory of non-equilibrium thermodynamics (Chen et al., 2013), is able to build a smooth link between geomechanics and other disciplines (e.g. geochemistry or microbiology). Mixture coupling theory was extended to unsaturated condition for HM coupling by Chen (Chen and Hicks, 2011), and the swelling effect was considered in coupled HM (Chen and Hicks, 2009) and HMC (Chen, 2013) frameworks. Moreover, chemical osmosis and thermo osmosis phenomena have been described in HMC (Chen and Hicks, 2013) and THM (Chen et al., 2013) frameworks. Dual-chemical osmosis within the HMC framework was also presented (Chen et al., 2018) .

In this paper, mixture coupling theory has been further extended to consider the influence of coupled swelling and dissolution/precipitation. Entropy is used to link the dynamic dissipation and energy function. The evolution of stress and pore volume fraction are obtained by analyzing the free energy density of the wetted matrix. Numerical simulations demonstrate the advantages of the new theoretical and mathematical formulations.

2 Balance equations and dissipative process

A microscopic domain V is selected within the material. It is assumed to be big enough to include solid, water and gas. S is the boundary attached to the solid phase and only fluid is allowed to pass through. The gas phase is assumed to be continuous with atmospheric pressure and p_{atm} is assumed to be zero to simplify the discussion (Neuman, 1975, Safai and Pinder, 1979).

2.1 Flux and density

The flux is defined as

$$\mathbf{I}^{\beta} = \rho^{\beta}(\mathbf{v}^{\beta} - \mathbf{v}^{s}) \tag{1}$$

where $\mathbf{I}^{\beta}$, $\mathbf{v}^{\beta}$, and ρ^{β} are the flux, velocity and density ("mixture density": mass in per unit mixture volume), respectively. β represents different fluid components: $\beta = w$ denotes water, $\beta = c$ denotes chemical (solute).

The fluid "true mass density" (the concentration in mass per unit volume fluid) is defined as

$$\rho_f^{\beta} = m^{\beta} / V_{fluid} \tag{2}$$

in which ρ^{β} is related to ρ_f^{β} through

$$\rho^{\beta} = S^{f}\phi\rho_f^{\beta} \tag{3}$$

where S^{f} is the saturation of pore fluid, ϕ is the porosity.

The total pore-fluid mixture density (e.g. water and a chemical) can be defined as:

$$\rho^{f} = \rho^{w} + \rho^{c} \tag{4}$$

and the barycentric velocity of the fluids can be defined as

$$\mathbf{v}^{f} = \left(\rho^{w} / \rho^{f}\right)\mathbf{v}^{w} + \left(\rho^{c} / \rho^{f}\right)\mathbf{v}^{c} \tag{5}$$

The diffusion flux of the water and chemical, which is relative to the barycentric motion, can be written as

$$\mathbf{J}^{\beta} = \rho^{\beta}(\mathbf{v}^{\beta} - \mathbf{v}^{f}) \tag{6}$$

by introducing the equation (1), the relationship between $\mathbf{J}^{\beta}$ and $\mathbf{I}^{\beta}$ can be obtained as

$$\mathbf{J}^{\beta} = \mathbf{I}^{\beta} - \rho^{\beta}(\mathbf{v}^{f} - \mathbf{v}^{s}) \tag{7}$$

where $\mathbf{v}^{s}$ is the velocity of the solid.

2.2 Balance equations

(1) *Energy balance*: Helmholtz free energy combines both internal energy and entropy (Haase, 1990). The balance equation can be derived based on the assumption of ignoring gas transport, as (Chen, 2013, Chen and Hicks, 2009)

$$\frac{D}{Dt}\int_V \psi dV = \int_S \boldsymbol{\sigma}\mathbf{n}\cdot\mathbf{v}^s dS \; - \int_S \mu^w \mathbf{I}^w \cdot \mathbf{n} dS - \int_S \mu^c \mathbf{I}^c \cdot \mathbf{n} dS - T\int_V \gamma dV \tag{8}$$

where the material time derivative is

$$\frac{D}{Dt} = \partial_t + \mathbf{v}^s \cdot \nabla \tag{9}$$

In equations (8), ψ is the Helmholtz free energy density, $\boldsymbol{\sigma}$ is the Cauchy stress tensor, $\mathbf{v}^s$ is the velocity of the solid, T is temperature, γ is the entropy production per unit volume, ∂_t is the time derivative and ∇ is the gradient.

The derivative version of the equation (8) is expressed as

$$\dot{\psi} + \psi\nabla\cdot\mathbf{v}^s - \nabla\cdot(\boldsymbol{\sigma}\mathbf{v}^s) + \nabla\cdot(\mu^w\mathbf{I}^w) + \nabla\cdot(\mu^c\mathbf{I}^c) = -T\gamma \le 0 \tag{10}$$

(2) The general balance equation for mass can be written as

$$\frac{D}{Dt}\left(\int_V \rho^\beta dV\right) = -\int_S \mathbf{I}^\beta \cdot \mathbf{n} dS + \int_V \dot{m}_r^\beta dV \tag{11}$$

where $-\int_S \mathbf{I}^\beta \cdot \mathbf{n} dS$ represents the mass change due to transport through the boundary and $\int_V \dot{m}_r^\beta dV$ represents the mass change due to reaction inside the system.
According to equation (11), the balance equation for water mass and chemicals are:

Water balance: The balance equation for the water mass (assuming water change due to reaction is negligible):

$$\frac{D}{Dt}\left(\int_V \rho^w dV\right) = -\int_S \mathbf{I}^w \cdot \mathbf{n} dS \tag{12}$$

and the derivative version is

$$\dot{\rho}^w + \rho^w\nabla\cdot\mathbf{v}^s + \nabla\cdot\mathbf{I}^w = 0 \tag{13}$$

Chemical balance: considering a mineral reaction process (e.g. $v_b B \rightleftarrows v_c C$) the chemical component C in the solution will be either generated due to dissolution of mineral B or consumed due to precipitation (reverse process). The balance equation for the chemical component is

$$\frac{D}{Dt}\left(\int_V \rho^c dV\right) = -\int_S \mathbf{I}^c \cdot \mathbf{n} dS + \int_V \dot{m}_r dV \tag{14}$$

The derivative version of the equation (14) is

$$\dot{\rho}^c + \rho^c \nabla \cdot \mathbf{v}^s + \nabla \cdot \mathbf{I}^c - \dot{m}_r = 0 \tag{15}$$

where m_r is the source term, representing the generation or consumption of the chemical specie. m_r can be written as

$$m_r = \nu_c M_c \xi \tag{16}$$

where ξ (number of moles per unit volume) is the extent of reaction, ν_c is the stoichiometric coefficient (positive for dissolution and negative for precipitation), and M_c is the molar mass of the *C*.

The time derivation of ξ can be linked to the dissolution/precipitation rate through

$$r = \nu_c \dot{\xi} \tag{17}$$

where r is dissolution rate.

2.3 Dissipative progress and dissolution entropy

The entropy change of the system could be categorized as: (1) the friction generated at the solid/water boundary; (2) the diffusion of chemical species; (3) the dissolution or precipitation induced entropy. Therefore, the dissipation can be obtained by using non-equilibrium thermodynamics, and the entropy production function is described as (Katachalsky and Curran, 1965)

$$0 \le T\gamma = -\mathbf{I}^w \cdot \nabla \mu^w - \mathbf{I}^c \cdot \nabla \mu^c + \dot{\eta} \tag{18}$$

where $\dot{\eta}$ represents the entropy change due to dissolution/precipitation. To simply the discussion, the chemical entropy change influence on fluid transport is neglected (e.g. chemical osmosis and $\dot{\eta} = 0$), so that the basic Darcy's law can be obtained through using phenomenological equations, as (Chen, 2013):

$$\mathbf{u} = -\frac{\mathbf{K} k_{rw}}{\mu} \nabla p_f \tag{19}$$

where $\mathbf{u}$ is Darcy's velocity, $\mathbf{K}$ is the permeability, k_{rw} is the relative permeability, and p_f is the pore fluid pressure.

The diffusion flux is (Chen and Hicks, 2013)

$$\mathbf{J}^c = -\rho_f D \nabla w^c \tag{20}$$

where ρ_f is the fluid mass density, D is the diffusion coefficient, and w^c is the mass fraction of the chemical component.

3 State equations for swelling and dissolution/precipitation

There are two types of water in a swelling/dissolving rock: 1) water in the pores which can be described using non-equilibrium thermodynamics, and 2) water in the clay platelets which is subjected to strong intermolecular and surface forces such that thermodynamics is not applicable (Israelachvili, 1991) (Figure 1). The solids can be classed as two types: 1) the solid structure, which follows the continuum thermodynamics (mechanics) and 2) the dissolved solids in the pore space, which do not support the structure strength (Figure 1).

3.1 Helmholtz free energy of pore fluid

Based on classical thermodynamics, the Helmholtz free energy density of the pore fluid ψ_{pore} can be written as

$$\psi_{pore} = -p^f + \rho_f^w \mu^w + \rho_f^c \mu^c \tag{21}$$

where $\rho_f^\beta = m^\beta / V_{fluid}$, denotes the density of liquid component per unit volume liquid. p^f is the fluid pressure in the pore space (the gas has been ignored). The time derivative of equation (21) leads to

$$\dot{\psi}_{pore} = -\dot{p}^f + \dot{\rho}_f^w \mu^w + \rho_f^w \dot{\mu}^w + \dot{\rho}_f^c \mu^c + \rho_f^c \dot{\mu}^c \tag{22}$$

According to the Gibbs-Duhem equation in constant temperature as

$$\dot{p}^f = \rho_f^w \dot{\mu}^w + \rho_f^c \dot{\mu}^c \tag{23}$$

and substituting equation (23) into equation (22) gives

$$\dot{\psi}_{pore} = \dot{\rho}_f^w \mu^w + \dot{\rho}_f^c \mu^c \tag{24}$$

3.2 Basic equation for deformation

The rock is assumed to maintain mechanical equilibrium so that $\nabla \cdot \boldsymbol{\sigma} = 0$. With the entropy production (18) and balance equation (10), the balance equation for ψ can be obtained as

$$\dot{\psi} + \psi \nabla \cdot \mathbf{v}^s - \left(\boldsymbol{\sigma} : \nabla \mathbf{v}^s \right) + \mu^w \nabla \cdot \mathbf{I}^w + \mu^c \nabla \cdot \mathbf{I}^c = 0 \tag{25}$$

To measure the rock's deformation state, classic continuum mechanics are considered here: An arbitrary reference configuration $\mathbf{X}$ is selected and at the time t its position is $\mathbf{x}$. some basic expressions (Wriggers, 2008):

$$\mathbf{F} = \frac{\partial \mathbf{x}}{\partial \mathbf{X}}\left(\mathbf{X}, t\right), \mathbf{E} = \frac{1}{2}\left(\mathbf{F}^{\mathbf{T}}\mathbf{F} - \mathbf{I}\right), \mathbf{T} = J\mathbf{F}^{-1}\boldsymbol{\sigma}\mathbf{F}^{-T}, J = dV / dV_0 \ , \ \dot{J} = J\nabla \mathbf{v}_s \tag{26}$$

where $\mathbf{E}$ is the Green strain, $\mathbf{F}$ is the deformation gradient, $\mathbf{I}$ is a unit tensor. $\mathbf{T}$ is the second Piola-Kirchhoff stress and $\boldsymbol{\sigma}$ is the Cauchy stress.

From equation (25), by using the mass balance equation(13), (15), and the mechanical relationship (26), it leads to:

$$\dot{\Psi} = tr(\mathbf{T}\dot{\mathbf{E}}) + \mu^w \dot{m}^w + \mu^c \dot{m}^c - \mu^c \dot{m}_r \tag{27}$$

$$\Psi = J\psi \ , \quad m^k = J\rho^k = JS^f \phi \rho_f^k \tag{28}$$

where Ψ is the free energy in the reference configuration, m^k ($k = w, c$)is the mass density of the fluid component in the reference configuration, and S^f is the saturation of pore fluid.

3.3 Free energy density of the wetted mineral matrix

Because the free energy of the mineral matrix is inclusive of fluid 'bound' between platelets which does not follow non-equilibrium thermodynamics, the free energy of the mineral matrix can be obtained by subtracting two parts from the total free energy of the combined solids/fluids system Ψ, including: (1) $J\phi^w \psi_{pore}$ due to the pore water and (2) the part of solid that dissolved from the solid matrix.

Therefore, from equation (21), (24), (27) and (28), the free energy density of the residual wetted mineral matrix is written as:

$$\dot{(\Psi - J\phi^w \psi_{pore})} = tr(\mathbf{T}\dot{\mathbf{E}}) + \bar{p}\dot{\upsilon} + \mu^w \dot{m}_{bound} - \mu^c \dot{m}_r \tag{29}$$

where $\bar{p} = S^f p^f$ is the average pressure in the pore space, $\upsilon = J\phi$ is denoted as the pore volume per unit referential volume, $m_{bound} = m^w - JS^f \phi \rho_f^w$ is denoted as the referential mass density of bound water.

For the reason of convenience, the dual potential (deformation energy) can be expressed as

$$W = (\Psi - J\phi^w \psi_{pore}) - \bar{p}\upsilon - \mu^w m_{bound} + \mu^c m_r \tag{30}$$

where W is a function of $\mathbf{E}$, $\bar{p}$, μ^w, μ^c. The expressions for $\mathbf{T}$, υ, m_{bound}, and m_r can be given.

Equation (30) implies the time derivative of $W(\mathbf{E}, \bar{p}, \mu^w, \mu^c)$ satisfies the relation

$$\dot{W}(\mathbf{E}, \bar{p}, \mu^w, \mu^c) = tr(\mathbf{T}\dot{\mathbf{E}}) - \dot{\bar{p}}\upsilon - \dot{\mu}^w m_{bound} + \dot{\mu}^c m_r \tag{31}$$

Note: the variable for the reaction part in equation (31) is the chemical potential variation $\dot{\mu}^c$. This variable is not widely used as most dissolution/precipitation research focuses on dissolution/precipitation rate rather than the change of chemical potential. Using Legendre transforms leads to

$$\dot{\mu}^c m_r = \left(\mu^c m_r\right)^{\cdot} - \mu^c \dot{m}_r \tag{32}$$

Invoking equation (32) into equation (31) leads to

$$\dot{W}(\mathbf{E}, \bar{p}, \mu^w, \mu^c) - \left(\mu^c m_r\right)^{\cdot} = tr(\mathbf{T}\dot{\mathbf{E}}) - \dot{\bar{p}}\upsilon - \dot{\mu}^w m_{bound} - \dot{m}_r \mu^c \tag{33}$$

Substituting $W_0 = W - \mu^c m_r$, which can be expressed as total deformation energy considering reaction induced energy, into equation (33) leads to

$$\dot{W}_0(\mathbf{E}, \bar{p}, \mu^w, m_r) = tr(\mathbf{T}\dot{\mathbf{E}}) - \dot{\bar{p}}\upsilon - \dot{\mu}^w m_{bound} - \dot{m}_r \mu^c \tag{34}$$

or

$$\dot{W}_0(\mathbf{E}, \bar{p}, \mu^w, m_r) = \left(\frac{\partial W_0}{\partial E_{ij}}\right)_{\bar{p}, \mu^w, m_r} \dot{E}_{ij} + \left(\frac{\partial W_0}{\partial \bar{p}}\right)_{E_{ij}, \mu^w, m_r} \dot{\bar{p}} + \left(\frac{\partial W_0}{\partial \mu^w}\right)_{E_{ij}, \bar{p}, m_r} \dot{\mu}^w + \left(\frac{\partial W_0}{\partial m_r}\right)_{E_{ij}, \bar{p}, \mu^w} \dot{m}_r \tag{35}$$

Therefore,

$$T_{ij} = \left(\frac{\partial W_0}{\partial E_{ij}}\right)_{\bar{p}, \mu^w, m_r},\ \upsilon = -\left(\frac{\partial W_0}{\partial \bar{p}}\right)_{E_{ij}, \mu^w, m_r},\ m_{bound} = -\left(\frac{\partial W_0}{\partial \mu^w}\right)_{E_{ij}, \bar{p}, m_r},\ \mu^c = -\left(\frac{\partial W_0}{\partial m_r}\right)_{E_{ij}, \bar{p}, \mu^w} \tag{36}$$

If equation (36) is differentiated respect to time, the fundamental constitutive equations for the evolution of stress, pore volume fraction, and the mass densities in the bound water and chemical potential can be obtained

$$\dot{T}_{ij} = L_{ijkl}\dot{E}_{kl} - M_{ij}\dot{\bar{p}} + S_{ij}\dot{\mu}^w - H_{ij}\dot{m}_r \tag{37}$$

$$\dot{\upsilon} = M_{ij}\dot{E}_{ij} + Q\dot{\bar{p}} + B\dot{\mu}^w + D\dot{m}_r \tag{38}$$

$$\dot{m}_{bound} = -S_{ij}\dot{E}_{ij} + B\ \dot{\bar{p}} + Z\dot{\mu}^{w} + X\ \dot{m}_{r} \tag{39}$$

$$\dot{\mu}^{c} = H_{ij}\dot{E}_{ij} + D\dot{\bar{p}} + X\dot{\mu}^{w} + Y\dot{m}_{r} \tag{40}$$

where the parameters L_{ijkl}, M_{ij}, S_{ij}, H_{ij}, B, X Y, Z are defined as the following group of equations:

$$\begin{aligned}
L_{ijkl} &= \left(\frac{\partial T_{ij}}{\partial E_{kl}}\right)_{\bar{p},\mu^{w},m_{r}} = \left(\frac{\partial T_{kl}}{\partial E_{ij}}\right)_{\bar{p},\mu^{w},m_{r}} \\
M_{ij} &= -\left(\frac{\partial T_{ij}}{\partial \bar{p}}\right)_{E_{ij},\mu^{w},m_{r}} = \left(\frac{\partial \upsilon}{\partial E_{ij}}\right)_{\bar{p},\mu^{w},m_{r}} \\
S_{ij} &= \left(\frac{\partial T_{ij}}{\partial \mu^{w}}\right)_{E_{ij},\bar{p},m_{r}} = -\left(\frac{\partial m_{bound}}{\partial E_{ij}}\right)_{\bar{p},\mu^{w},m_{r}} \\
H_{ij} &= -\left(\frac{\partial T_{ij}}{\partial m_{r}}\right)_{E_{ij},\bar{p},\mu^{w}} = \left(\frac{\partial \mu^{c}}{\partial E_{ij}}\right)_{\bar{p},\mu^{w},m_{r}} \\
B &= \left(\frac{\partial \upsilon}{\partial \mu^{w}}\right)_{E_{ij},\bar{p},\mu^{c}} = \left(\frac{\partial m_{bound}}{\partial \bar{p}}\right)_{E_{ij},\mu^{w},m_{r}} \\
Z &= -\left(\frac{\partial m_{bound}}{\partial \mu^{w}}\right)_{E_{ij},\bar{p},m_{r}}, \quad Q = \left(\frac{\partial \upsilon}{\partial \bar{p}}\right)_{E_{ij},\mu^{w},m_{r}} \\
Y &= \left(\frac{\partial \mu^{c}}{\partial m_{r}}\right)_{E_{ij},\bar{p},\mu^{w}}, \quad X = \left(\frac{\partial m_{bound}}{\partial m_{r}}\right)_{E_{ij},\bar{p},\mu^{w}} = \left(\frac{\partial \mu^{c}}{\partial m_{r}}\right)_{E_{ij},\bar{p},\mu^{w}}
\end{aligned} \tag{41}$$

4 Coupled hydro-mechanical-chemical constitutive equations

4.1 Mechanical behaviour

Equations (37), (38), (39) and (40) give the general coupled equations for mechanical behaviour, porosity, mass density of the bounded water and chemical potential of the fluid component. These equations are for non-linear, large deformation, and anisotropic conditions. As the attention of this article is focused on the coupled dissolution and swelling influence, a few assumptions are made including (Chen & Hicks, 2013):

i) Small strains assumption that leads to the replacement of the Green Strain tensor E_{ij} by the strain tensor ε_{ij}, and the Piola-Kirchhoff stress T_{ij} by the Cauchy stress σ_{ij}.

ii) The parameters L_{ijkl}, M_{ij}, S_{ij}, Z, B, and Q are material-dependent constants and the material is isotropic, therefore, the tensors M_{ij}, S_{ij} and H_{ij} are diagonal and can be written in the forms of scalars ζ, ω_s and ω_R, as

$$M_{ij} = \zeta\delta_{ij} \ , \ S_{ij} = \omega_s\delta_{ij}, H_{ij} = \omega_R\delta_{ij} \tag{42}$$

Based on assumption ii), the elastic stiffness L_{ijkl} can be a fourth-order isotropic tensor:

$$L_{ijkl} = G(\delta_{ik}\delta_{jl} + \delta_{il}\delta_{jk}) + (K - \frac{2G}{3})\delta_{ij}\delta_{kl} \tag{43}$$

Here, G denotes the material's shear modulus and K denotes the bulk modulus.

With the assumptions i), ii), the governing stress equation (37) can be simplified to

$$\dot{\sigma}_{ij} = (K - \frac{2G}{3})\dot{\varepsilon}_{kk}\delta_{ij} + 2G\dot{\varepsilon}_{ij} - \zeta\dot{\bar{p}}\delta_{ij} + \omega_s\dot{\mu}^w\delta_{kl} - \omega_R\dot{m}_r\delta_{kl} \tag{44}$$

where the quantity ζ is related to the bulk modulus K and K_s in a manner from poroelasticity through the equation $\zeta = 1-(K/K_s)$. In this equation, the two terms (ω_s and ω_R) have been introduced. They represent two coefficients related to swelling and reactive dissolution/precipitation process.

The term $\omega_R\dot{m}_r\delta_{kl}$ is interpreted as the stress change coefficient due to dissolution/precipitation. Since ω_R is related to the bulk modulus K, it can be expressed as $\omega_R = \omega_r K$. The dissolution/precipitation induced stress as

$$\dot{\sigma}_r = \omega_r K\dot{m}_r \tag{45}$$

Equation (45) can be compared with the thermal-induced stress as (Xia et al., 2014):

$$\dot{\sigma}_T = \alpha_T K\dot{T} \tag{46}$$

where α_T is the thermal expansion coefficient of the solid grains.

Substituting equation(45) into equation (44), the constitutive equation for solids deformation can be obtained as

$$\dot{\sigma}_{ij} = (K - \frac{2G}{3})\dot{\varepsilon}_{kk}\delta_{ij} + 2G\dot{\varepsilon}_{ij} - \zeta\dot{\bar{p}}\delta_{ij} + \omega_s\dot{\mu}^w\delta_{kl} - \omega_r K\dot{m}_r\delta_{kl} \quad (47)$$

Assuming mechanical equilibrium ($\partial\sigma_{ij}/\partial x_j = 0$), and using displacement variables $d_i (i = 1,2,3)$ through $\varepsilon_{ij} = \frac{1}{2}(d_{i,j} + d_{j,i})$, and introducing equation (23), equation (47) leads to

$$G\nabla^2\dot{\mathbf{d}} + \left(\frac{G}{1-2\theta}\right)\nabla(\nabla\cdot\dot{\mathbf{d}}) - (\zeta - \frac{\omega_s}{S^f\rho_f^w})\nabla\dot{\bar{p}} - \omega_r K\nabla\dot{m}_r = 0 \quad (48)$$

where θ is the Poisson's ratio, $\bar{p} = S^f p^f$ is the average pore pressure and its time derivative is (Lewis and Schrefler, 1987)

$$\dot{\bar{p}} = S^f\frac{\partial p^f}{\partial t} + \frac{C_s}{\phi}p^f\frac{\partial p^f}{\partial t} = (S^f + \frac{C_s}{\phi}p^f)\frac{\partial p^f}{\partial t},$$

in which C_s in the specific moisture content.

Equation (48) can then be rewritten as:

$$G\nabla^2\dot{\mathbf{d}} + \left(\frac{G}{1-2\theta}\right)\nabla(\nabla\cdot\dot{\mathbf{d}}) - (\zeta - \frac{\omega_s}{S^f\rho_f^w})\nabla\left[(S^w + \frac{C_s}{\phi}p^f)\dot{p}^f\right] - \omega_r K\nabla\dot{m}_r = 0 \quad (49)$$

Equation (49) presents a general formula including the influence of both the swelling and dissolution/precipitation on mechanical behaviour.

Consider the relationship in equation (16), the governing equation for both swelling and dissolution is

$$G\nabla^2\dot{\mathbf{d}} + \left(\frac{G}{1-2\theta}\right)\nabla(\nabla\cdot\dot{\mathbf{d}}) - (\zeta - \frac{\omega_s}{S^f\rho_f^w})\nabla\left[(S^w + \frac{C_s}{\phi}p^f)\dot{p}^f\right] - \omega_d\nu_c M_c K\nabla\dot{\xi} = 0 \quad (50)$$

And the governing equation for both swelling and precipitation is

$$G\nabla^2\dot{\mathbf{d}} + \left(\frac{G}{1-2\theta}\right)\nabla(\nabla\cdot\dot{\mathbf{d}}) - (\zeta - \frac{\omega_s}{S^f\rho_f^w})\nabla\left[(S^w + \frac{C_s}{\phi}p^f)\dot{p}^f\right] + \omega_p\nu_c M_c K\nabla\dot{\xi} = 0 \quad (51)$$

where ω_d and ω_p are the dissolution and precipitation coefficient, respectively.

4.2 Fluid-phase

From equation (3), the water density equation (13) and the Euler identity, the conservation equation of water is obtained as

$$(S^f \upsilon \rho_f^w)^{\cdot} + \nabla \cdot (\rho_f^w \mathbf{u}) = 0 \tag{52}$$

From equations (52), (10), (19) and(38), it leads to

$$\begin{aligned} & S^f \rho_f^w \zeta \nabla \cdot \dot{\mathbf{d}} + S^f \rho_f^w (Q + B^D / \rho_f^w) \dot{\bar{p}} \\ & + \phi \rho_f^w \frac{\partial S^f}{\partial t} + \phi S^f \frac{\partial \rho_f^w}{\partial t} + \rho_f^w \left[-\mathrm{k} \frac{k_{rw}}{\mu} \nabla^2 p_f \right] = 0 \end{aligned} \tag{53}$$

Considering the rate of change of saturation function and the rate of change of water density function (Lewis and Schrefler, 1987)

$$\phi \frac{\partial S^f}{\partial t} + \frac{\phi S^f}{\rho_f^w} \frac{\partial \rho_f^w}{\partial t} = C_S \frac{\partial p^f}{\partial t} + \phi \frac{S^f}{K_w} \frac{\partial p^f}{\partial t} = (C_S + \phi \frac{S^f}{K_w}) \frac{\partial p^f}{\partial t} \tag{54}$$

Equation (53) can be rewritten as

$$-\mathrm{k} \frac{k_{rw}}{\mu} \nabla^2 p_f + (C_S + \phi \frac{S^f}{K_w}) \frac{\partial p^f}{\partial t} + S^f (Q + B^D / \rho_f^w)(S^f + \frac{C_s}{\phi} p^f) \frac{\partial p^f}{\partial t} + S^f \zeta \nabla \cdot \dot{\mathbf{d}} = 0 \tag{55}$$

4.3 Chemical-phase

From the partial mass equation (11), (13), (15) and the mass density equation (3), by introducing equation (7) and using the Euler identity, it leads to

$$(S^f \upsilon \rho_f^\beta)^{\cdot} + J \nabla \cdot (\rho^\beta \mathbf{u}) + J \nabla \cdot \mathbf{J}^\beta = \dot{m}_r^\beta \tag{56}$$

If the fluid is assumed to be incompressible, by introducing the mass fraction $w^\beta = \rho_f^\beta / \rho_f$, it leads to

$$(S^f \upsilon \rho_f^f w^\beta)^{\cdot} + \nabla \cdot (\rho_f^f w^\beta \mathbf{u}) + \nabla \cdot \mathbf{J}^\beta = \dot{w}_r^\beta \tag{57}$$

where $w_r^\beta = m_r^\beta / \rho_f$ for mass fraction of the reaction amount.

Because $\sum_\beta w^\beta = 1$ and $\sum_\beta \mathbf{J}^\beta = 0$, summing over all the fluid components leads to the relationship

$$(\upsilon S^f \rho_f)^{\cdot} + \nabla \cdot (\rho_f \mathbf{u}) = \dot{m}_r^\beta \tag{58}$$

By invoking equation(58), equation (56) can be transformed to give

$$(\upsilon S^f \rho_f) \dot{w}^\beta + \rho_f \mathbf{u} \cdot \nabla \dot{w}^\beta + \nabla \cdot \mathbf{J}^\beta = \dot{m}_r^\beta \tag{59}$$

Because the dissolution/precipitation rate deals with mole concentration, with the relationship $w^\beta = \frac{c^\beta M_\beta}{\rho}$, equation (59) can be converted from mass fraction to mole concentration:

$$(\upsilon S^f \rho_f) \dot{c}^\beta + \rho_f \mathbf{u} \cdot \nabla \dot{c}^\beta + \nabla \cdot \mathbf{J}^\beta = r^\beta \tag{60}$$

where c^{β} is the mole concentration of fluid component, and r^{β} is the dissolution/precipitation rate (moles per unit volume per unit time).

From equations (20) and (60), the chemical transport equation can be obtained as

$$S^{f}\phi\dot{c}^{\beta}-\left(k\frac{k_{rw}}{\mu}\nabla p^{f}\right)\cdot\nabla c^{\beta}-D\nabla^{2}c^{\beta}=r^{\beta} \tag{61}$$

4.4 Equation validation

Equations (49), (55) and (61) represent the coupled mechanical, hydraulic, and chemical process. The swelling and dissolution/precipitation influence, namely, $\frac{\omega_s}{S^f\rho_f^w}$ and ω_d/ω_p, have been incorporated into the coupled HMC framework. The new governing equations are a further extension of Chen's research (Chen, 2013), with considering the dissolution/precipitation influence. If the swelling and dissolution terms are ignored, the developed equations will be simplified to the governing equations proposed by Lewis (Lewis and Schrefler, 1987).

The dissolution part in equation (51) (or more general equation (47)) has the same equation stress-strain relationship as in the literature (Coussy, 2004, Zhang and Zhong, 2018, Zhang and Zhong, 2017) with a rigorous mathematical derivation and further consideration of swelling/precipitation. Note: The name of the variable such as 'dissolution parameter' for consistency with 'swelling parameter' in this paper, with 'reaction dilation coefficient' or 'chemical dilation coefficient' in references (Coussy, 2004, Zhang and Zhong, 2018)

5 Numerical simulation

5.1 Numerical model

The clay-rich rocks, which are used as part of the engineered barrier for nuclear waste disposal, will encounter the influences of swelling and dissolution/precipitation when in contact with hyper-alkaline leachates generated from the cement materials around the nuclear waste. (Note: In a geological disposal facility (GDF), cement and bentonite being in direct contact may be limited to plugs and / or seals, including borehole seals (a direct interaction), although leachate from cementitious backfill material used in association with one waste category could indeed

migrate in groundwater to bentonite buffer material being used in another part of the GDF in association with a different waste category: an indirect interaction). In this section, a simple numerical simulation is presented to show the role of swelling and dissolution/precipitation in a coupled HMC process.

5.1.1 Geometry and boundary condition

Conceptual model: Figure 2 shows the prescribed geometry and boundary conditions, which represent a geomaterial sample around the nuclear waste container.

Boundary condition: In this model, boundary A is free and permeable, while boundary B is fixed and permeable. The upper and lower boundaries are fixed and non-permeable so that no vertical displacement is allowed and no water passes through. At boundary B, water pressure decreases to -10 MPa at the start of the simulation.

Initial condition: The whole domain is assumed to be at mechanical equilibrium, with zero effective stress throughout. The domain initially contains water at a pressure of -5 MPa and a saturation degree of 0.995, according to van Genuchten's model, given by

$$k_{rw} = \left(S^w\right)^{0.5}\left[1-\left(1-\left(S^w\right)^{1/m}\right)^m\right]^2$$

$$S^w = \left[\left(-P/M\right)^{1/(1-m)}+1\right]^{-m}$$

Chemical condition: In the numerical simulation, it is assumed that quartz is the major mineral component of rock/clay, which will first form H_4SiO_4 (solid) with water, and then react with hyper-alkaline leachate from the cement as (Haxaire and Djeran-Maigre, 2009)

$$\underset{solid}{H_4SiO_4} + \underset{liquid}{2OH^-} = \underset{liquid}{H_2SiO_4^{2-}} + \underset{liquid}{2H_2O}$$

The dissolution rate equation is (Savage et al., 2002)

$$r = k_{rate}A\left(1-\left(\frac{Q}{K_{eq}}\right)^{\theta}\right)^n \tag{62}$$

in which r is the dissolution rate in moles per unit volume porous media, k_{rate} is the rate constant, A is reactive surface area per unit volume of porous media, Q is the ion activity product, θ is a 'coefficient related to the stoichiometry of the reaction that forms an activated

complex, but is often set to be 1'(Savage et al., 2002), n is an empirical coefficient that is assumed to be 1 in this paper, and K_{eq} is the thermodynamic equilibrium constant described as

$$K_{eq} = \frac{\left[H_2SiO_4^{2-}\right]_{eq}}{\left[OH^-\right]_{eq}^2} \tag{63}$$

in which $\left[H_2SiO_4^{2-}\right]_{eq}$ is the concentration of $H_2SiO_4^{2-}$ and $\left[OH^-\right]_{eq}$ is the concentration of OH^- at equilibrium, respectively. Since K_{eq} is a constant value, $\left[H_2SiO_4^{2-}\right]_{eq}$ and $\left[OH^-\right]_{eq}$ will influence each other, i.e. the higher $\left[OH^-\right]_{eq}$ is, the higher $\left[H_2SiO_4^{2-}\right]_{eq}$ will be. So in the numerical simulation, not only are the conditions for H_2SiO_4 required, but also the conditions for OH^-.

Chemical boundary and initial condition (H_2SiO_4): The concentration of H_2SiO_4 on boundary A is set to be $0.003 mol/L$ (t>0) to represent the H_2SiO_4 brought by the external groundwater. The domain contains no H_2SiO_4 initially, but the mineral will react with the hyper-alkaline leachates at t>0, and the concentration of OH^- from the hyper-alkaline leachates is $0.3 mol/L$ (pH=13.48) an applied all the domain (t=0).

Other parameters in this modelling study adopted from literature(Ziefle et al., 2018, Lichtner and Seth, 1996, Hu et al., 2012, Savage et al., 2002) and listed in Table 1.

5.1.2 Simulation procedure

The swelling term $\frac{\omega_s}{S^f \rho_f^w}$ and the dissolution/precipitation term ω_d may be complicated expressions. To simplify the discussion, the swelling coefficient is assumed to be $\frac{\omega_s}{S^f \rho_f^w} = 0.2$.

The strain resulting from dissolution can be expressed by considering the volumetric strain (Tao et al., 2019) as

$$\varepsilon_d = \frac{V_s^{rem}}{V_s^{ini}} - 1 = -\frac{M_b}{\rho_t^b}\frac{d(n)}{V_s} = -\frac{M_b}{\rho_t^b}\frac{1}{1-\phi}\frac{d(n)}{V} \tag{64}$$

where n is the change of the number of moles, V_s is the volume of the solid part, V is the total volume, M_b is the mole mass of mineral B, and ρ_t^b is the true mass density of mineral B.

If the dissolution rate is defined as the number of moles per unit time per unit volume of porous media as in equation (62), $\frac{d(n)}{V}$ in equation (64) becomes the reaction extent ξ. From the stress-strain relationship (47) with consideration of dissolution influence only, the corresponding stress-strain relationship (assuming the solid is homogeneous and linearly elastic) can be obtained as

$$\sigma_d = -K\varepsilon_d = -K\frac{M_b}{\rho_t^b}\frac{1}{1-\phi}\frac{d(n)}{V} = -\omega_d K m_d \tag{65}$$

With equation (65) and the relationship in equation (16), it leads to

$$\omega_d = \frac{1}{\nu M_c}\frac{M_b}{\rho_t^b}\frac{1}{1-\phi} \tag{66}$$

For example: Considering quartz (e.g. H_4SiO_4), as the density is 1800g/m^3 and molar mass 96g/mol, using equation (66) leads to $\omega_d = \frac{5.3E-4}{(1-\phi)\nu}$. The variable in equation (65) is m_d rather than ξ. In Equation (50), the variable has been switched to ξ, the coefficient before ξ changes to $\omega_d \nu_c M_c = \frac{5.3E-5}{(1-\phi)}$, which is a similar value as the 'reaction dilation coefficient'(1E-5) in recent literature (Zhang and Zhong, 2018).

To obtain a deep understanding of the influence caused by swelling and dissolving/precipitating, four scenarios are considered in the numerical simulation:

i). "No swelling and no dissolution". In this scenario, the influence of swelling or dissolution is not considered, this situation becomes the classic theory described by Lewis's research (Lewis and Schrefler, 1987).

ii). "Swelling only". In this scenario, only the influence of swelling is considered, this is the same as Chen's research (Chen, 2013).

iii). "Dissolution only".

iv). "Swelling and dissolution".

Note: By setting the dissolution parameter to be negative, the influence of precipitation can be analyzed.

5.2 1D numerical results

Figure 3 shows the distribution of pore water pressure along the middle line of the sample under the four scenarios at different time. The water pressure distributions in these scenarios are the same. This is because the porosity evolution, the water loss in the pore space due to swelling is ignored and the osmosis phenomena induced by chemical concentration variation are not considered to simplify the discussion. Figure 3 shows that the pressure in the domain decreases gradually with time, and reaches equilibrium at t=1000h. Owing to the van Genuchten relationship between water pressure and saturation, the distribution of saturation (Figure 4) shows a similar trend as the pressure distribution in Figure 3.

Figure 5 shows the horizontal displacements according to the four scenarios at 240 hours and 600 hours. The displacement in the scenario i and iii looks like the "same", and means that dissolution has 'no' contribution to displacement. However, this is because the dissolution rate is so slow that the amount of quartz dissolved within 600 hours is very small. The contribution of dissolution on displacement is very limited, even not in the same magnitude with the contribution of water pressure, so there is no significant influence of dissolution displayed in Figure 5. This also explains why the displacement in scenario ii and iv is the same. Comparing scenario i and ii, when there is only the influence of swelling, the displacement is significantly decreased, which means that swelling has a negative influence on the consolidation process.

Because water pressure reaches equilibrium around 1000 hours, water pressure or swelling will no longer contribute to the displacement change after 1000 hours. The displacement change after 1000 hours is purely caused by dissolution. In Figure 8, at t=2000h, dissolution slightly enlarges the displacement, and at a longer time, the displacement is further enlarged. Consider the conclusion from Figure 5, it is clear that swelling and dissolution has an opposite influence of displacement.

Figure 7 shows the H_2SO_4 concentration distribution with time. At the early stage, the concentration near boundary A is dominated by diffusion, whereas the concentration in the domain is dominated by the dissolution of quartz. As time increases, at t=120hours, the concentration near boundary A exceeds the initial value (0.003 mol/L) due to the combined influence of dissolution and diffusion, however, the concentration in the domain is still

dominated by dissolution, because the diffusion toward the boundary B is slow. Later, the concentration in the domain exceeds the value on the boundary A and the diffusion direction reverse from B to A.

Figure 8 presents the influence of precipitation on horizontal displacement. Compared with Lewis' research(Lewis and Schrefler, 1987), precipitation and dissolution have opposite influences. This is because, theoretically, precipitation can be viewed as an opposite process of dissolution.

5.3 2D numerical results

The above 1D numerical simulation presents the influence of swelling and dissolution/precipitation on mechanical behaviour. In this section, a simple 2D model is presented for engineering applications. The basic parameters and boundaries are the same as the 1D model. The difference is that the pressure at the domain and the left boundary varies linearly from -5MPa to -10MPa, representing the pressure variation in a natural situation (Figure 9). At the start of the simulation, the pressure at the right-hand boundary drops by -5MPa to simulate pressure change caused by engineering disturbance (e.g. excavation).

The displacement distribution is presented in Figure 10. From (a) and (b), it can be found that at t=240h, the displacement in the "swelling only" situation is smaller than the displacement in "no swelling/dissolution" situation, which means the swelling process has a negative influence on displacement. From (a) and (c), dissolution has a very small influence on displacement as dissolution is kinetically controlled so that it doesn't show influence in such a short time. Comparing (c) and (d) at a much longer time (e.g. 20000hours), the influence of dissolution becomes much more significant. This reveals the importance of including chemical reactions in the long term analysis for chemical disturbed soils/rocks.

5.4 Discussion and limitations

This research is a further extension of Biot's theory by incorporating the influence of swelling and dissolution/precipitation. The specific attention is paid on the chemical influence on mechanical behaviour. A group of general fully cross-coupling equations have been obtained in equations (37), (38), (39) and (40), and a further simplified equation for small strains are obtained in equations (44).

There are a few limitations of this research (mainly for numerical modelling):

1. As the attention of this paper has been focused on embedding the coupling of swelling and dissolution/precipitation terms into an HMC framework, the change of physical properties (e.g. permeability, bulk modulus) are ignored in the numerical simulation. But all of these physical properties can be incorporated in the final new constitutive equations.
2. The clay-rich sample considered in this research is idealized and is assumed to be homogeneous.
3. The water loss into the clay platelet is ignored. The osmosis phenomenon, induced by chemical components in the pore water, is not considered.
4. The swelling and dissolution/precipitation terms (e.g. $\frac{\omega_s}{S^f \rho_f^w}$, ω_d etc.) need to be determined by further experimental research.

6 Conclusion

In this paper, mixture coupling theory has been extended to derive a new coupled hydro-mechanical-chemical formulation accounting for the complex molecular-scale swelling and dissolution/precipitation interactions. The distributions of pore water pressure, degree of water saturation, and displacement have been analysed using numerical simulations under various scenarios for swelling/dissolution/precipitation. The results demonstrate that molecular-scale interactions can have a significant influence on the macro-scale physical deformation. This indicates that molecular-scale influence should be sufficiently considered in the design of engineered barriers or a safety analysis of the natural barriers for waste management (e.g. nuclear waste disposal).

This paper is focused on the theoretical and numerical study, and the swelling and dissolution/precipitation parameters need to be determined by further experimental research.

Acknowledgement:

The first, second and fourth authors would like to thank the CERES studentship support from the University of Leeds. The third and fifth authors would like to thank the Welsh European Funding Office, Grant/Award Number: FLEXIS.

Reference:

Adler, M, Mäder, UK,Waber, HN 1999. High-Ph Alteration of Argillaceous Rocks: An Experimental Study. *Schweizerische Mineralogische und Petrographische Mitteilungen,* 79**,** 445-454.

Anderson, R, Ratcliffe, I, Greenwell, H, Williams, P, Cliffe, S,Coveney, P 2010. Clay Swelling—a Challenge in the Oilfield. *Earth-Science Reviews,* 98**,** 201-216.

Berner, U 1992. Evolution of Pore Water Chemistry During Degradation of Cement in a Radioactive Waste Repository Environment. *Waste Management,* 12**,** 201-219.

Berner, U 1998. Geochemical Modelling of Repository Systems: Limitations of the Thermodynamic Approach. *Radiochimica Acta,* 82**,** 423-428.

Biot, MA 1962. Mechanics of Deformation and Acoustic Propagation in Porous Media. *Journal of applied physics,* 33**,** 1482-1498.

Biot, MA,Temple, G 1972. Theory of Finite Deformations of Porous Solids. *Indiana University Mathematics Journal,* 21**,** 597-620.

Chen, X. 2010. *Unsaturated Hydro-Chemo-Mechanical Modelling Based on Modified Mixture Theory.* PhD, The University of Manchester (PhD thesis).

Chen, X 2013. Constitutive Unsaturated Hydro-Mechanical Model Based on Modified Mixture Theory with Consideration of Hydration Swelling. *International Journal of Solids and Structures,* 50**,** 3266-3273.

Chen, X,Hicks, MA 2009. Influence of Water Chemical Potential on the Swelling of Water Sensitive Materials. *Computers & structures,* 88**,** 1498-1505.

Chen, X,Hicks, MA 2011. A Constitutive Model Based on Modified Mixture Theory for Unsaturated Rocks. *Computers and Geotechnics,* 38**,** 925-933.

Chen, X,Hicks, MA 2013. Unsaturated Hydro-Mechanical-Chemo Coupled Constitutive Model with Consideration of Osmotic Flow. *Computers and Geotechnics,* 54**,** 94-103.

Chen, X, Pao, W,Li, X 2013. Coupled Thermo-Hydro-Mechanical Model with Consideration of Thermal-Osmosis Based on Modified Mixture Theory. *International Journal of Engineering Science,* 64**,** 1-13.

Chen, X, Thornton, SF,Pao, W 2018. Mathematical Model of Coupled Dual Chemical Osmosis Based on Mixture-Coupling Theory. *International Journal of Engineering Science,* 129**,** 145-155.

Coussy, O 2004. *Poromechanics*, John Wiley & Sons.

Criscenti, L,Serne, R 1988. Geochemical Analysis of Leachates from Cement/Low-Level Radioactive Waste/Soil Systems. Pacific Northwest Lab., Richland, WA (USA).

Gens, A, Guimarães, LdN, Olivella, S,Sánchez, M 2004. Analysis of the Thmc Behaviour of Compacted Swelling Clay for Radioactive Waste Isolation. *Elsevier Geo-Engineering Book Series,* 2**,** 317-322.

Haase, R 1990. *Thermodynamics of Irreversible Processes,* New York, Dover.

Haxaire, A,Djeran-Maigre, I 2009. Influence of Dissolution on the Mechanical Behaviour of Saturated Deep Argillaceous Rocks. *Engineering geology,* 109**,** 255-261.

Heidug, W,Wong, SW 1996. Hydration Swelling of Water‐Absorbing Rocks: A Constitutive Model. *International Journal for Numerical and Analytical Methods in Geomechanics,* 20**,** 403-430.

Hu, D, Zhou, H, Hu, Q, Shao, J, Feng, X,Xiao, H 2012. A Hydro-Mechanical-Chemical Coupling Model for Geomaterial with Both Mechanical and Chemical Damages Considered. *Acta Mechanica Solida Sinica,* 25**,** 361-376.

Israelachvili, JN 1991. *Intermolecular and Surface Forces,* London, Academic Press.
Jia, Y, Bian, H, Xie, S, Burlion, N,Shao, J 2017. A Numerical Study of Mechanical Behavior of a Cement Paste under Mechanical Loading and Chemical Leaching. *International Journal for Numerical and Analytical Methods in Geomechanics,* 41**,** 1848-1869.
Katachalsky, A,Curran, PF 1965. *Nonequilibrium Thermodynamics in Biophysics,* Cambridge, MA, Harvard University Press.
Lewis, RW,Schrefler, BA 1987. *The Finite-Element Method in Deformation and Consolidation of Porous Media,* New York, Wiley.
Lichtner, P,Seth, M 1996. User's Manual for Multiflo: Part Ii Multiflo 1.0 and Gem 1.0 Multicomponent-Multiphase Reactive Transport Model. *Southwest Research Institute*.
Liu, Y, Wang, J, Zhao, X, Ke, D, Xie, J, Cao, S, Ma, L, Jiang, W,Chen, L. Design and Development of a Large-Scale Thmc Experiment of Compacted Bentonite for Geological Disposal of High Level Radioactive Waste in China. 12th ISRM Congress, 2011. International Society for Rock Mechanics.
Madsen, FT,Müller-Vonmoos, M 1989. The Swelling Behaviour of Clays. *Applied Clay Science,* 4**,** 143-156.
Neuman, SP 1975. Galerkin Approach to Saturated–Unsaturated Flow in Porous Media. *In:* GALLAGHER, R. H., ODEN, J. T., TAYLOR, C. & ZIENKIEWICZ, O. C. (eds.) *Finite Elements in Fluids.* New York: John Wiley & Sons.
Peter, GJ. Application of Coupled Thermo-Hydro-Mechanical-Chemical (Thmc) Processes in Hydrothermal Systems to Processes near a High-Level Nuclear Waste Repository. ASME 2011 14th International Conference on Environmental Remediation and Radioactive Waste Management, 2011. American Society of Mechanical Engineers, 737-745.
Safai, NM,Pinder, GF 1979. Vertical and Horizontal Land Deformation in a Desaturating Porous Medium. *Adv. Water Res.,* 2**,** 19-25.
Savage, D, Noy, D,Mihara, M 2002. Modelling the Interaction of Bentonite with Hyperalkaline Fluids. *Applied Geochemistry,* 17**,** 207-223.
Schwartzentruber, J, Fürst, W,Renon, H 1987. Dissolution of Quartz into Dilute Alkaline Solutions at 90 C: A Kinetic Study. *Geochimica et Cosmochimica Acta,* 51**,** 1867-1874.
Tao, J, Wu, Y, Elsworth, D, Li, P,Hao, Y 2019. Coupled Thermo-Hydro-Mechanical-Chemical Modeling of Permeability Evolution in a Co2-Circulated Geothermal Reservoir. *Geofluids,* 2019.
Terzaghi, K 1943. Theory of Consolidation. *Theoretical Soil Mechanics***,** 265-296.
Wriggers, P 2008. *Nonlinear Finite Element Methods*, Springer Science & Business Media.
Xia, T, Zhou, F, Liu, J, Kang, J,Gao, F 2014. A Fully Coupled Hydro-Thermo-Mechanical Model for the Spontaneous Combustion of Underground Coal Seams. *Fuel,* 125**,** 106-115.
Xiaodong, L, Prikryl, R,Pusch, R 2011. Thmc-Testing of Three Expandable Clays of Potential Use in Hlw Repositories. *Applied Clay Science,* 52**,** 419-427.
Zhang, X,Zhong, Z 2017. A Thermodynamic Framework for Thermo-Chemo-Elastic Interactions in Chemically Active Materials. *SCIENCE CHINA Physics, Mechanics & Astronomy,* 60**,** 084611.
Zhang, X,Zhong, Z 2018. Thermo-Chemo-Elasticity Considering Solid State Reaction and the Displacement Potential Approach to Quasi-Static Chemo-Mechanical Problems. *International Journal of Applied Mechanics,* 10**,** 1850112.
Ziefle, G, Matray, J-M, Maßmann, J,Möri, A 2018. Coupled Hydraulic-Mechanical Simulation of Seasonally Induced Processes in the Mont Terri Rock Laboratory (Switzerland). *Mont Terri Rock Laboratory, 20 Years.* Springer.

TABLE 1 Material parameters (Ziefle et al., 2018).

Parameters	Physical meaning	Values and units
ρ_t^w	Density of fluid	1000kg/m^3
ϕ	Porosity	0.16
k	permeability	6.8E-20m^{-2}
μ	Dynamics viscosity	1e-3Pa*s
m	van Genuchten parameter	0.54
M	van Genuchten parameter	44.4MPa
G	Shear modulus	1.2GPa
θ	Poisson's ratio	0.18
ζ	Biot's coefficient	1
D	Diffusion coefficient	1E-9 m^2/s (Lichtner and Seth, 1996b)
Q	Compressibility	5E-10
k_{rate}	Reactive surface area	2.102E-10mol/m^2/s (Hu et al., 2012)
A	Reactive surface area	9.53E3m^2/m (Savage et al., 2002)
K_{eq}	Equilibrium constant	1E-4

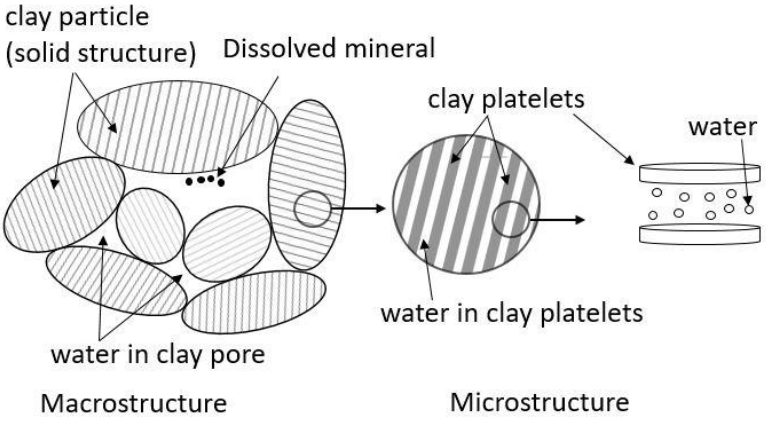

FIGURE 1 Water types and solid types

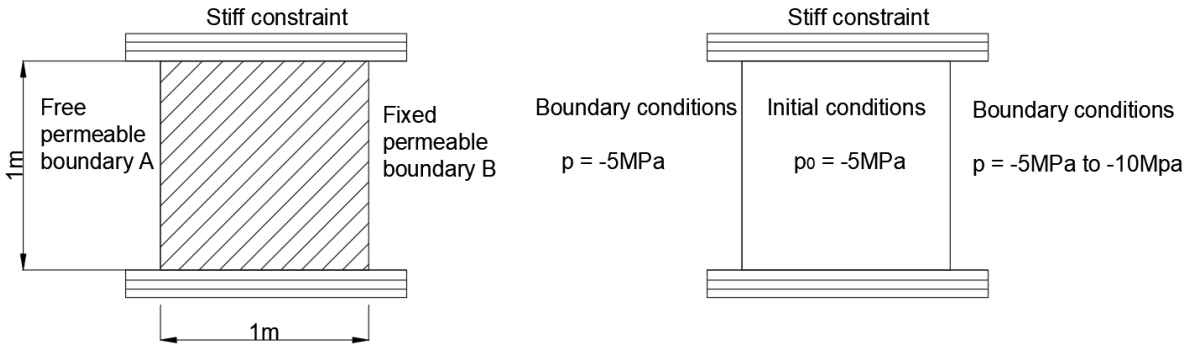

FIGURE 2 Geometry and Boundary condition

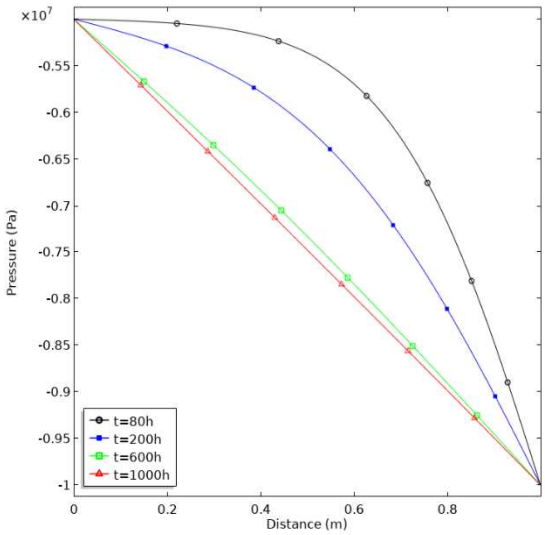

FIGURE 3 Distribution of pore water pressure (scenario i, ii, iii, iv)

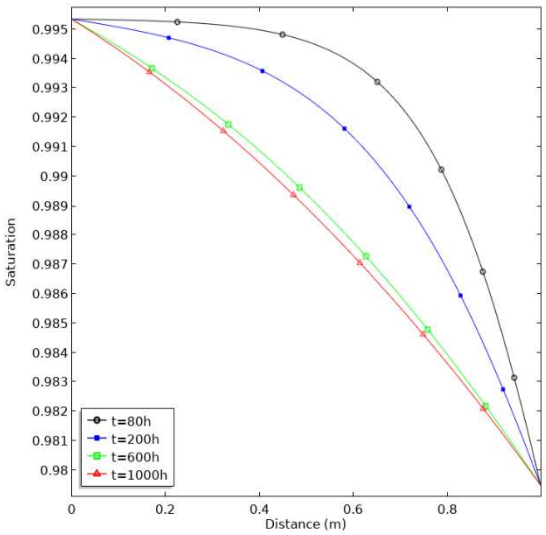

FIGURE 4 Distribution of saturation (scenario i, ii, iii, iv)

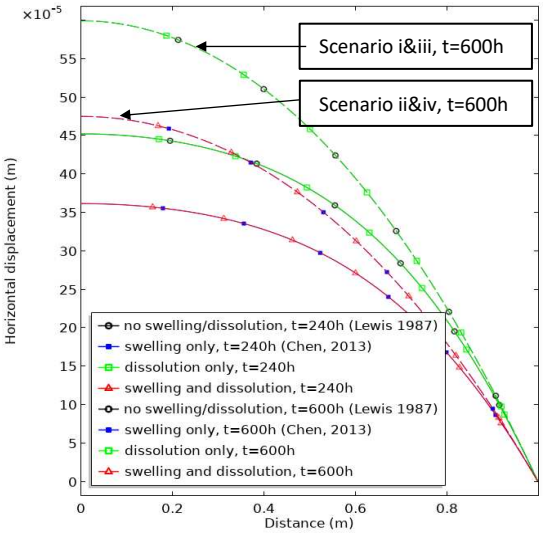

FIGURE 5 Horizontal displacement (short time)

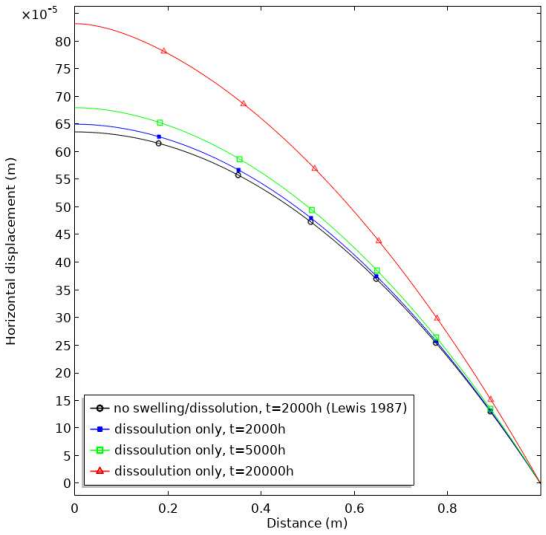

FIGURE 6 Horizontal displacement (long time)

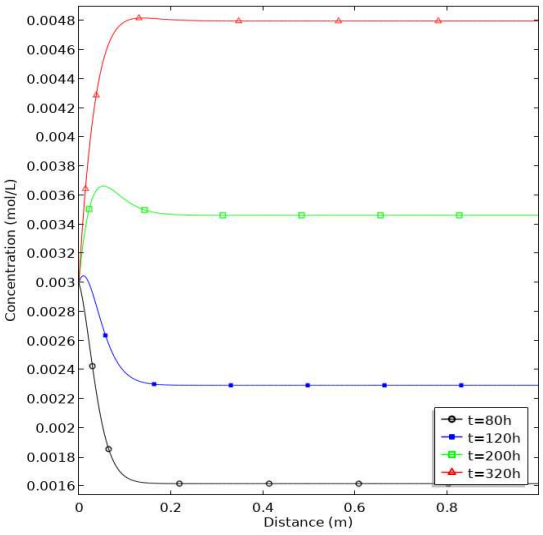

FIGURE 7 H2SO4 concentration

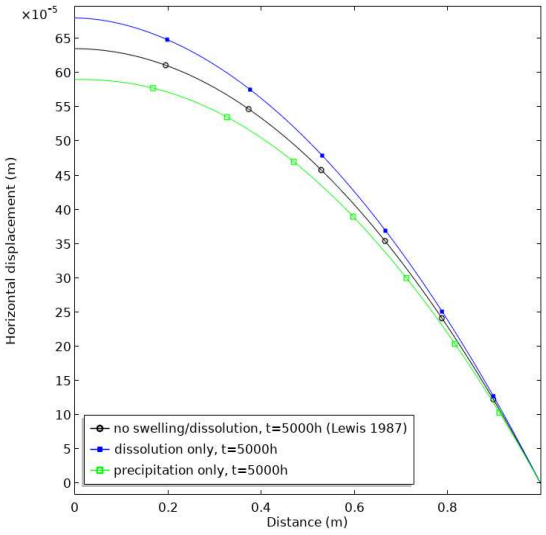

FIGURE 8 Horizontal displacement (dissolution and precipitation)

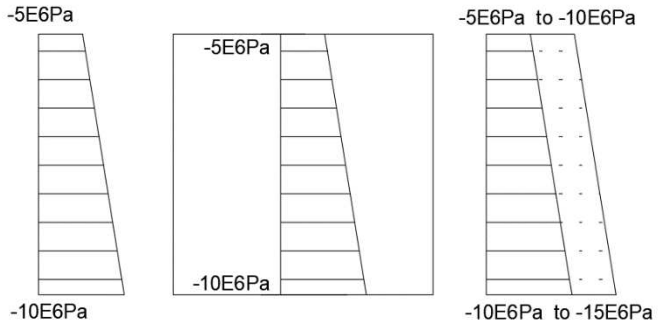

FIGURE 9 Pressure condition in 2D model

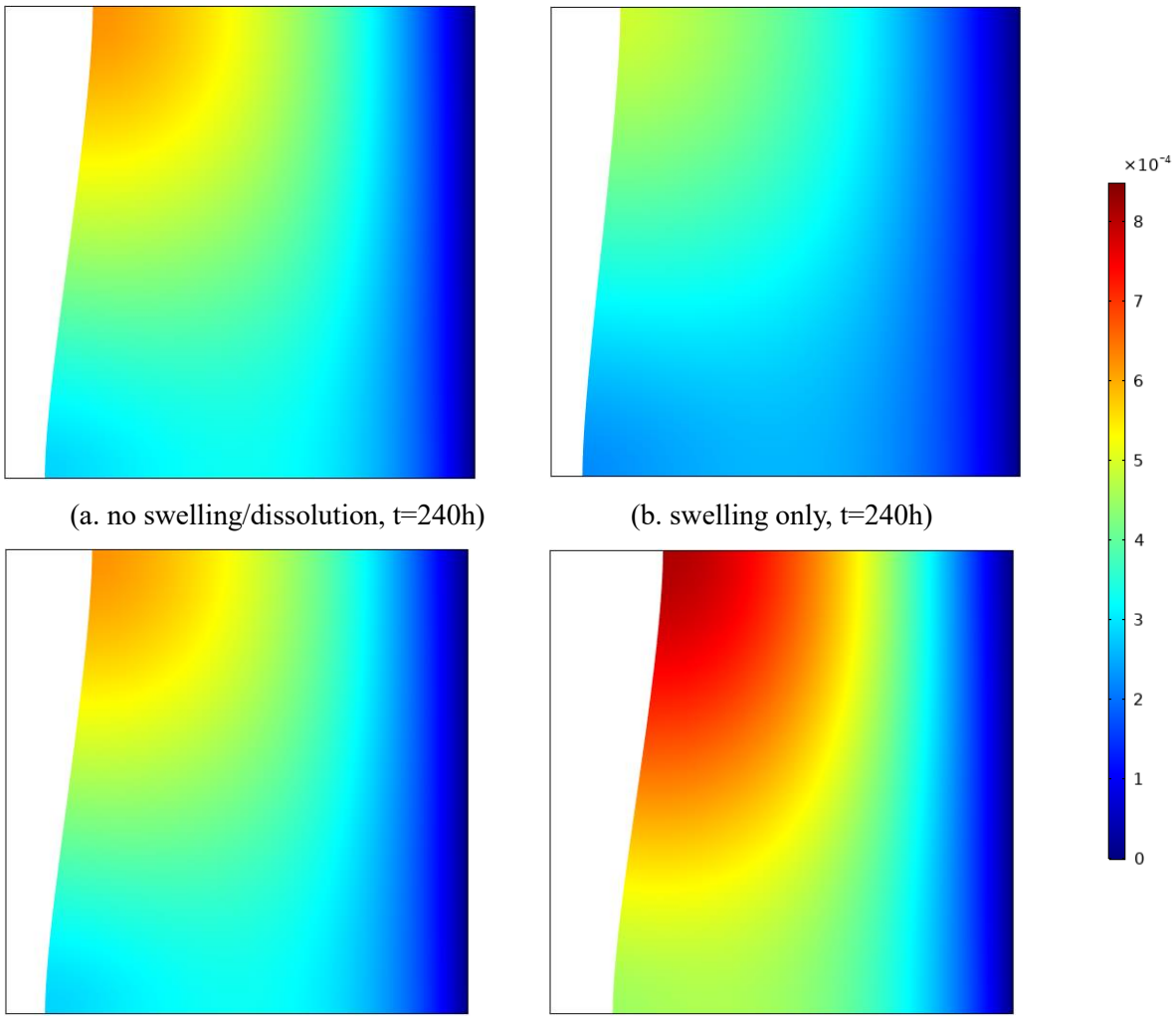

(a. no swelling/dissolution, t=240h) (b. swelling only, t=240h)

(c. dissolution only, t=240h) (d. dissolution only, t=20000h)

FIGURE 10 Horizontal displacement distribution in different situations (unit: m)